Organic LETTERS

Letter

pubs.acs.org/OrgLett

Key Structural Elements for Cellular Uptake of Acinetobactin, a Major Siderophore of *Acinetobacter baumannii*

Woon Young Song,[†,§] Dawa Jeong,[†,§] Jimin Kim,[†] Min Wook Lee,[†] Man Hwan Oh,[‡] and Hak Joong Kim*[,†]

[†]Department of Chemistry, Korea University, 145 Anam-ro, Seongbuk-gu, Seoul 02841, Republic of Korea

[‡]Department of Nanobiomedical Science, Dankook University, Cheonan 31116, Republic of Korea

Supporting Information

ABSTRACT: Acinetobactin is a major siderophore utilized by the human pathogen *Acinetobacter baumannii*. The rapid acquisition of drug resistance by *A. baumannii* has garnered concern globally. Herein, acinetobactin and systematically generated analogues were prepared and characterized; the binding and cellular delivery of Fe(III) by the analogues were evaluated. This investigation not only led to the clarification of the physiologically relevant acinetobactin structure but also revealed several key structural elements for its functionality as a siderophore.

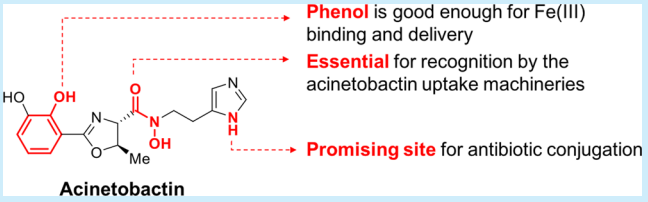

The rapid and global dissemination of drug-resistant strains of *Acinetobacter baumannii* has garnered considerable concern, particularly in nosocomial settings.[1] Currently, polymyxins are considered the sole effective means to treat this deadly pathogen, but their nephrotoxicity limits their therapeutic usage.[1] Thus, the development of a novel and safe treatment option to address this medical challenge is urgently needed.

The siderophore−antibiotic conjugate (SAC) strategy is a targeted drug delivery approach in which siderophores are utilized as delivery vectors, thus allowing the uptake of conjugated antibiotic molecules into bacterial cells through dedicated siderophore receptors.[2] The distinctive cellular uptake mechanism of SACs, which is independent of the conventional porin-mediated pathway, renders this strategy an effective means to overcome the drug resistance of *A. baumannii* because reduced porin expression is a significant contributor to the resistance of *A. baumannii*.[3]

Three siderophores have been identified from *A. baumannii*.[4] Among them, acinetobactin (Figure 1, **1** and **2**) is the major siderophore found in most clinical *A. baumannii* isolates, and the cellular machinery associated with its utilization has been shown to be an essential virulence factor.[5] Thus, acinetobactin appears to be the ideal choice as a delivery vector for *A. baumannii*-targeting SACs. The structure of acinetobactin was originally proposed as **1**,[4a] but Walsh et al. subsequently proposed an alternative structure, **2**, whose biosynthetic formation involves the spontaneous rearrangement of the oxazolinyl hydroxamate core of **1** to isoxazolidinone.[6] While the more physiologically relevant form has yet to be elucidated, Wencewicz et al. recently proposed an intriguing "pH-triggered swapping" mechanism, where the pH of the medium is the key determinant of the utilized form of acinetobactin.[7] For the design of optimal SAC structures targeting *A. baumannii*, it is crucial to clarify the siderophore form and to understand how it interacts with the relevant cellular uptake machineries. Toward this end, we herein describe the systematic generation and characterization of acinetobactin analogues to elucidate key structural elements of acinetobactin to function as a siderophore.

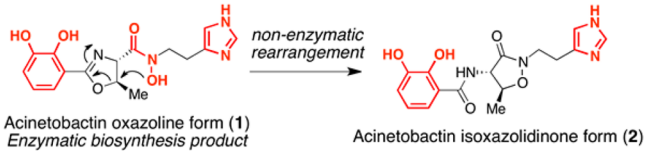

Figure 1. Structures of siderophores used by *A. baumannii*. Potential iron chelating motifs are shown red.

First, the acinetobactins (**1** and **2**)[8] were characterized. Kinetic experiments on the conversion from **1** to **2** showed that the rearrangement is pH-dependent, indicating that the protonation state of the hydroxamate in **1** is critical (k = 0.024 min^{-1} at pH 7.5 vs no conversion at pH 4.2) (Figure S1). The modest reaction rate at a neutral pH ($t_{1/2}$ = 29 min) suggests that the formation of **2** under physiological settings is marginally feasible.

To function as a siderophore, a molecule must be capable of not only binding Fe(III) but also delivering Fe(III) inside the cell.[9] The Fe(III)-binding properties of **1** and **2** were assessed on the basis of the chrome azurol S (CAS) assay, as depicted in Figure 2A. Both compounds are capable of binding Fe(III) based on the color change of the dye from deep blue to orange. The oxazoline form (**1**) appears to form a slightly tighter

Received: December 9, 2016

DOI: 10.1021/acs.orglett.6b03671
Org. Lett. XXXX, XXX, XXX−XXX

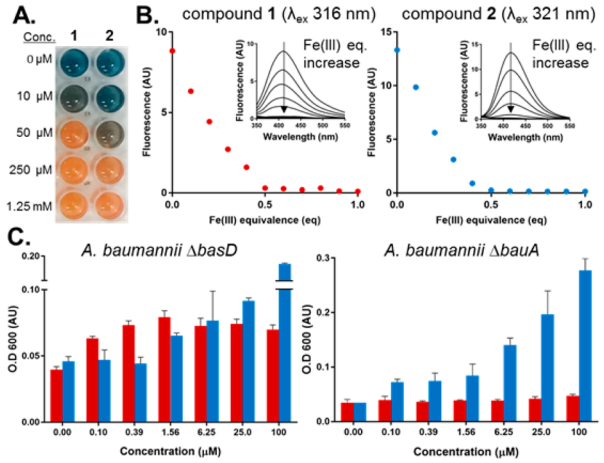

Figure 2. Characterization of two forms of acinetobactin, **1** and **2**. (A) Concentration-dependent chrome azurol S (CAS) assay. (B) Plots of the fluorescence titration results for **1** (10 μM) and **2** (10 μM) with Fe(acac)$_3$ in methanol. (C) *A. baumannii* ATCC 19606 Δ*basD* and Δ*bauA* growth promotion assays employing **1** (red) and **2** (blue) (Luria–Bertani media, 200 μM 2,2′-bipyridyl, 12 h culture at 37 °C).

Fe(III) complex than **2** because it has induced a color change at a lower concentration (50 μM). To determine the binding stoichiometry of the resulting Fe(III)–acinetobactin complexes, the fluorescence of **1** and **2** alone and in the presence of Fe(III) was evaluated. As shown in Figure 2B, the fluorescence of both compounds was completely quenched upon addition of 0.5 equiv of Fe(III), which indicates the formation of 2:1 complexes between **1** or **2** and Fe(III) and suggests that the binding mode of these compounds with Fe(III) was similar. Both forms of acinetobactin are likely to utilize common ligating motifs, namely the catechol dihydroxyl groups and one of the imidazole amines, to fulfill the optimal hexacoordinate octahedral geometry of the corresponding Fe(III) complexes. This suggests that the hydroxamate moiety of **1**, another potential metal binding motif, is not directly involved in the complexation with Fe(III).

To evaluate whether **1** and **2** are capable of delivering Fe(III) intracellularly, growth promotion assays were conducted. In these experiments, each compound was used to treat an iron-deficient culture of *A. baumannii* ATCC 19606 Δ*basD* or Δ*bauA* mutant, in which the gene for the production or uptake of acinetobactin was deleted, respectively.[10] When the Δ*basD* mutant was used in the assay, oxazoline **1** appeared to promote cellular growth more efficiently at lower concentrations (≤1.56 μM), while isoxazolidinone **2** prevailed at higher concentrations (>6.25 μM) (Figure 2C). When the Δ*bauA* mutant was used in the assay, the activity of **1** was completely abolished, indicating that the cellular uptake of **1** was dependent on the acinetobactin receptor, BauA. Interestingly, however, the cultures treated with **2** could grow efficiently and in a concentration-dependent fashion. The BauA-independent Fe(III) delivery by **2** is unexpected. Currently, we speculate that this event could be porin-mediated, or it might occur via passive diffusion delivery of the Fe(III)–**2** complex; the clarification of the mechanism would require further analyses.[11] These observations strongly indicate that oxazoline **1** is the physiologically relevant siderophore structure for *A. baumannii*, rather than **2**, because the specificity of a key acinetobactin uptake receptor, BauA, appears to have been evolved toward the former.

To systematically elucidate the key structural elements of **1** and **2** that affect their Fe(III) binding and cellular delivery, 10 novel analogues were generated. These analogues were designed with a specific focus on the modification of the iron-binding motifs; the synthetic route for the preparation of these compounds (**9a–j**) is presented in Scheme 1.

Scheme 1. Structures of Acinetobactin Analogues and Their Synthetic Routes

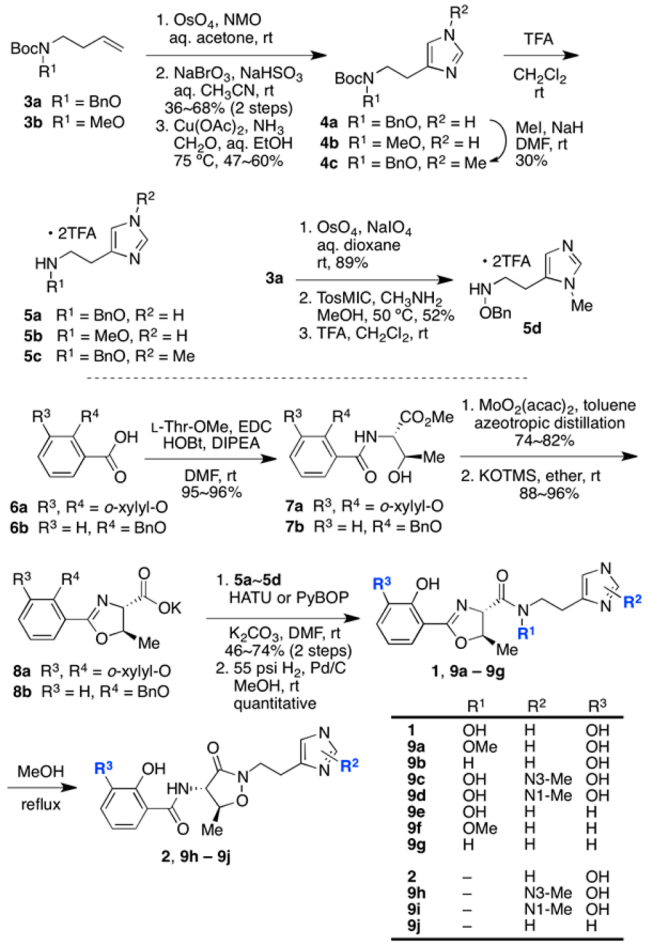

	R1	R2	R3
1	OH	H	OH
9a	OMe	H	OH
9b	H	H	OH
9c	OH	N3-Me	OH
9d	OH	N1-Me	OH
9e	OH	H	H
9f	OMe	H	H
9g	H	H	H
2	–	H	OH
9h	–	N3-Me	OH
9i	–	N1-Me	OH
9j	–	H	H

Briefly, the imidazole fragments (**5a–c**) were prepared from *N*,*O*-protected *N*-butenylhydroxylamines (**3a,b**) via Cu(II)-promoted de novo imidazole formation reactions.[12] The N^3-methyl group of **5c** could be readily introduced by a simple substitution reaction with methyl iodide (**4a** → **4c**). For the selective introduction of the methyl group at the N^1 position of **5d**, a van Leusen reaction employing toluenesulfonylmethyl isocyanide (TosMIC) and methylamine was adopted.[13] Construction of the oxazoline fragments was initiated by coupling the *O*-protected benzoic acid precursors (**6a,b**) with L-threonine methyl ester. Then, Ishihara's dehydrative cyclization protocol using a Mo(VI) oxide catalyst was applied to construct the oxazoline ring system,[14] and subsequent mild saponification using potassium trimethylsilanolate afforded the corresponding oxazoline fragments (**8a,b**) as the potassium carboxylate forms.[15]

Lastly, the unions between the imidazole and oxazoline fragments were effected using HATU or PyBOP as the amide-coupling agents; subsequent hydrogenolysis provided the oxazoline forms of acinetobactin and its analogues (**1**, **9a–g**).

DOI: 10.1021/acs.orglett.6b03671
Org. Lett. XXXX, XXX, XXX–XXX

Compounds **1** and **9c**–**e** were then heated in methanol to provide the corresponding isoxazolidinone derivatives (**2**, **9h**–**j**) via rearrangement reactions.

CAS assays were performed with these analogues in hand (Figure 3A). First, the role of the hydroxamate group of **1** in

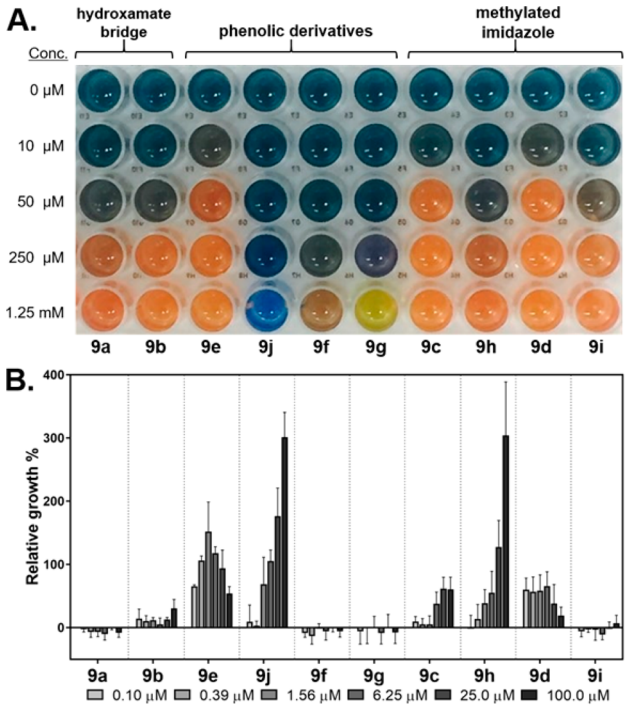

Figure 3. Functional characterization of 10 acinetobactin analogues: (A) CAS assay results; (B) growth promotion assay results using *A. baumannii* Δ*basD*.

iron binding was investigated using **9a** and **9b**. Although these analogues possess modifications that disrupt the metal binding of the hydroxamate (**9a**: *O*-methylation, **9b**: a simple amide linkage), both could elicit color changes in the CAS assay, indicating that they were capable of binding Fe(III). This observation was consistent with the proposed iron-binding mode of acinetobactin **1** involving the catechol dihydroxyl and imidazole groups, not the hydroxamate (vide supra).

Four phenolic derivatives (**9e**,**f**,**g**,**j**) were prepared and tested to investigate the role of the catechol moiety. Notably, these compounds comprise pseudomonine (**9j**), another siderophore produced by some *Pseudomonas* strains, and its analogues.[16] Prepseudomonine (**9e**) exhibited a strong CAS signal even at a low concentration (50 μM), indicating that the 3″-hydroxyl group of **1** is not critical for iron binding. This result is not unexpected because the phenolic oxazoline moiety is often found in other siderophores, such as mycobactin.[17] Modifications of the hydroxamate bridge in **9f** and **9g** appeared to considerably weaken the iron binding, contrary to that for the catechol siblings (**9a**,**b**). Surprisingly, pseudomonine (**9j**) failed to elicit a noticeable color change in the CAS assay, even at 1.25 mM, unlike **2**. Nevertheless, the fluorescence quenching of **9j** by Fe(III) was observed (Figure S3), which indicates that **9j** is still capable of binding Fe(III), albeit not tightly.

Analogues **9c**/**9h** and **9d**/**9i** were designed to identify which amine atom, N^1 or N^3, of the pendant imidazole ring is responsible for iron binding. Interestingly, the CAS assay results reveal that *N*-methylation did not significantly decrease the iron-binding propensity of any of these analogues, suggesting that the ethylene linker is flexible and thus well capable of positioning either amine atom toward the metal center.

A series of growth promotion assays were conducted with *A. baumannii* Δ*basD* to correlate the iron-binding abilities of the acinetobactin analogues to their iron delivery capabilities (Figure 3B).[18] Strikingly, hydroxamate-modified analogues **9a** and **9b** failed to exhibit growth promotion activities despite their Fe(III) binding capabilities. This observation implicates that although the hydroxamate bridge of **1** may not function as an iron chelator, it is a critical element for the recognition of acinetobactin (**1**) by the relevant cellular uptake machinery. At this point, it is uncertain which component (e.g., BauA, BauD, or BauF) would directly interact with the hydroxamate moiety; this will be investigated in due course.

The growth promotion activities of the prepseudomonine analogues (**9e**–**g**) well correlated with their iron-binding affinities; only prepseudomonine (**9e**) could act as a siderophore, and its activity was analogous to that of **1** at concentrations below 6.25 μM. Interestingly, pseudomonine (**9j**) could promote bacterial growth despite its weak Fe(III) binding, but this activity was BauA-independent, similar to **2** (Figure S5B). The imidazole-modified analogues exhibited somewhat complex results. Among the oxazoline analogues (**9c**,**d**), N^1-methylated **9d** showed an activity similar to that of **1**, while the activity of **9c** was much lower. This indicates that the conformation of the **9d**–Fe(III) complex is more compatible with the acinetobactin uptake system, and it also suggests that the N^1 position of **1** would be a suitable site for conjugating an antibiotic molecule. Among the isoxazolidinone analogues (**9h**,**i**), N^1-methylated **9i** was unable to promote growth of *A. baumannii*, while **9h** exhibited BauA-independent activities similar to those of **2** (Figure S5B).

Collectively, this study discloses the intriguing structure–function relationships of various acinetobactin analogues, and several crucial implications for the successful design of effective acinetobactin–antibiotic conjugates were derived. First, oxazoline **1** is likely the physiologically relevant siderophore structure for *A. baumannii* based on the growth-promotion assay results using mutant strains. This conclusion suggests that **1** would serve better as the antibiotic delivery vehicle targeting *A. baumannii*, as it more appropriately exploits the acinetobactin uptake machinery than **2**, the key requirement for conferring the anticipated potency and selectivity to the antibiotic conjugates based on acinetobactin.[2] As for the conjugate design, the hydroxamate bridge seems to be critical for cellular uptake because its modification (**9a** and **9b**) completely abolished iron delivery. In addition, the N^1 position of the pendant imidazole appears to be a promising drug conjugation site because modification at this site (**9d**) did not abrogate the iron delivery function. Notably, modification of N^1 can be easily introduced by applying the van Leusen reaction, as demonstrated herein.

The siderophore-based antibiotic delivery approach provides an alternative and powerful approach to overcome the threatening problems of drug resistance of various pathogens. The insights provided in this study will serve as an indispensable foundation for the success of ensuing efforts in this direction and may lead to the discovery of potent acinetobactin–antibiotic conjugates that will be effective in treating drug-resistant *A. baumannii*.

DOI: 10.1021/acs.orglett.6b03671
Org. Lett. XXXX, XXX, XXX–XXX

■ ASSOCIATED CONTENT

Supporting Information

The Supporting Information is available free of charge on the ACS Publications website at DOI: 10.1021/acs.orglett.6b03671.

Experimental procedures for characterization and synthesis as well as spectroscopic data of the compounds studied herein (PDF)

■ AUTHOR INFORMATION

Corresponding Author

*E-mail: hakkim@korea.ac.kr.

ORCID

Hak Joong Kim: 0000-0002-3213-2230

Author Contributions

§Y.W.S. and D.J. contributed equally to this work.

Notes

The authors declare no competing financial interest.

■ ACKNOWLEDGMENTS

This work was supported by a National Research Foundation of Korea (NRF) grant (Grant Nos. NRF-2012R1A1A1042665, NRF-2015R1D1A1A01056815, NRF20110020033, and NRF-2016R1C1B1016370). We also thank Ms. Hyun Hee Lee and Mr. Yunhwa Choi for their helpful assistance on the mass data collection and the hemolytic activity assay, respectively.

■ REFERENCES

(1) (a) Doi, Y.; Murray, G. L.; Peleg, A. Y. *Semin. Respir. Crit. Care Med.* **2015**, *36*, 85. (b) Dijkshoorn, L.; Nemec, A.; Seifert, H. *Nat. Rev. Microbiol.* **2007**, *5*, 939.

(2) (a) Johnstone, T. C.; Nolan, E. M. *Dalton Trans.* **2015**, *44*, 6320. (b) Górska, A.; Sloderbach, A.; Marszałł, M. P. *Trends Pharmacol. Sci.* **2014**, *35*, 442. (c) Ji, C.; Juárez-Hernández, R. E.; Miller, M. J. *Future Med. Chem.* **2012**, *4*, 297.

(3) Vila, J.; Marti, S.; Sanchez-Cespedes, J. *J. Antimicrob. Chemother.* **2007**, *59*, 1210.

(4) (a) Yamamoto, S.; Okujo, N.; Sakakibara, Y. *Arch. Microbiol.* **1994**, *162*, 249. (b) Proschak, A.; Lubuta, P.; Grün, P.; Löhr, F.; Wilharm, G.; De Berardinis, V.; Bode, H. B. *ChemBioChem* **2013**, *14*, 633. (c) Penwell, W. F.; DeGrace, N.; Tentarelli, S.; Gauthier, L.; Gilbert, C. M.; Arivett, B. A.; Miller, A. A.; Durand-Reville, T. F.; Joubran, C.; Actis, L. A. *ChemBioChem* **2015**, *16*, 1896.

(5) Gaddy, J. A.; Arivett, B. A.; McConnell, M. J.; Lopez-Rojas, R.; Pachon, J.; Actis, L. A. *Infect. Immun.* **2012**, *80*, 1015.

(6) (a) Sattely, E. S.; Walsh, C. T. *J. Am. Chem. Soc.* **2008**, *130*, 12282. (b) Wuest, W. M.; Sattely, E. S.; Walsh, C. T. *J. Am. Chem. Soc.* **2009**, *131*, 5056.

(7) Shapiro, J. A.; Wencewicz, T. A. *ACS Infect. Dis.* **2016**, *2*, 157.

(8) The preparation of **1** and **2** was previously reported by us. Kim, J.; Lee, J. E.; Ree, H.; Kim, H. J. *Bull. Korean Chem. Soc.* **2015**, *36*, 439.

(9) Miethke, M.; Marahiel, M. A. *Microbiol. Mol. Biol. Rev.* **2007**, *71*, 413.

(10) Oh, M. H.; Lee, J. C.; Kim, J.; Choi, C. H.; Han, K. *Appl. Environ. Microbiol.* **2015**, *81*, 3357.

(11) Recently, similar acinetobactin transporter-independent growth promotion of *Aeromonas salmonicida* by an analogue of **2** was reported by Jiménez and co-workers. In this study, the authors proposed the involvement of an unidentified alternative transporter. Balado, M.; Segade, Y.; Rey, D.; Osorio, C. R.; Rodríguez, J.; Lemos, M. L.; Jiménez, C. *ACS Chem. Biol.* **2016**, DOI: 10.1021/acschembio.6b00805.

(12) Totter, J. R.; Darby, W. J. *Org. Synth.* **1944**, *24*, 64.

(13) van Leusen, A. M.; Wildeman, J.; Oldenziel, O. H. *J. Org. Chem.* **1977**, *42*, 1153.

(14) Sakakura, A.; Umemura, S.; Ishihara, K. *Chem. Commun.* **2008**, 3561.

(15) Laganis, E. D.; Chenard, B. L. *Tetrahedron Lett.* **1984**, *25*, 5831.

(16) Anthoni, U.; Christophersen, C.; Nielsen, P. H. *J. Nat. Prod.* **1995**, *58*, 1786.

(17) Hider, R. C.; Kong, X. *Nat. Prod. Rep.* **2010**, *27*, 637.

(18) Growth inhibition observed at high concentrations of **9d** and **9e** seems to occur due to the Fe(III) sequestration from the medium, overwhelming the Fe(III) delivery effect by these molecules. Similar observations were reported by others, e.g.: Madsen, J. L. H.; Johnstone, T. C.; Nolan, E. M. *J. Am. Chem. Soc.* **2015**, *137*, 9117.

DOI: 10.1021/acs.orglett.6b03671
Org. Lett. XXXX, XXX, XXX−XXX